EVALUATION OF STRESS-STRAIN STATES IN CYLINDRICAL SHELLS WITH GEOMETRIC DISCONTINUITIES

Ion DURBACĂ[1], Gheorghe Cosmin CIOCOIU[2*], Nicoleta SPOREA[3*], Anca Mădălina DUMITRESCU[4]

The paper addresses the analytical and experimental evaluation of stress-strain states on the inner and outer surfaces of cylindrical shells with geometric discontinuities.

The purpose of this evaluation is to utilize theoretical and experimental methods to determine the equivalent stresses developed at the level of the analyzed cylindrical shells. The differences between the equivalent stress values obtained analytical and experimental, are attributed to the use of simplifying assumptions that do not fully correspond to reality.

Keywords: stresses, deformations, cylindrical shells, geometric discontinuities.

1. Introduction

In the composition of industrial process equipment predominates mechanical structures with revolution shells (spherical, cylindrical, conical, ellipsoidal, hyperboloidal, toroidal, toro-spherical, etc.) [1].

As a result of the technological processes that take place in these equipment by means of chemically and/or mechanically aggressive substances, damage to the components may occur, which is the essential reason why theoretical (analytical and numerical) as well as experimental methods must be developed for estimating the current stress-strain states. Such methods are also necessary for cylindrical shells with geometrical discontinuities or structural imperfections.

From the literature, it has been found that the study of mechanical structures with revolution shells has been oriented on addressing the following subjects, such as:

[1] Prof., Dept. of Equipment for Industrial Processes, National University of Science and Technology POLITEHNICA Bucharest, Romania

[2] Eng., Dept. of Equipment for Industrial Processes, National University of Science and Technology POLITEHNICA Bucharest, Romania

[3] Associate Professor, PhD, Dept. of Equipment for Industrial Processes, National University of Science and Technology POLITEHNICA Bucharest, Romania

[4] Associate Professor, PhD, Dept. of Equipment for Industrial Processes, National University of Science and Technology POLITEHNICA Bucharest, Romania

*Corresponding Authors: Gheorghe Cosmin CIOCOIU, Email: gheorghe.ciocoiu@upb.ro ; Nicoleta SPOREA, Email: nicoleta.sporea@upb.ro

strength analysis of cylindrical shells with tubular fittings [1]; design of pressure equipment without cracks, based on the analytical method, as well as with consideration of crack damage, based on the critical energy principle [2]; analysis of critical stresses specific to tubular structures - without and with cracks [3]; calculation of the damage of tubular structures based on the principle of critical energy [4] and superposition of effects [5]; experimental investigation of the stress and deformation state of prestressed cylindrical shells, taking into account temperature effects [6]; theoretical approach of analytical solutions for the bending of pressure vessel shells [7]; study of the regularity of the bending moments of the quasi-static evolution of perfectly elasto-plastic structures under the action of time-dependent mechanical stresses [8]; prediction of the service life of structures subjected to fatigue in order to verify the applied stresses as a function of the number of stress cycles [9]; experimental investigation of normal and residual stress states in branching elements of pipelines with geometric and structural discontinuities [10].

Therefore, the current approaches of the present work can justify the research carried out on the appropriateness and necessity of theoretical and experimental analysis on the evaluation of stress-strain states in a specific study of cylindrical shells provided with geometrical discontinuities.

2. Basic descriptive elements

For the analytical and experimental study, the model represented in Fig. 1, of a structure composed of cylindrical shells, provided with a geometric discontinuity is considered.

The analyzed model has the following geometrical and mechanical characteristics:

- inner pressure; $p_i = 3MPa$;

- weldless, hot-rolled pipe, construction material - P265GH, according to SR EN 10216-2;

- length of the cylindrical elements, L_j [m]: L_1 = 0.07 m; L_2 = 0.05 m; L_3 = 0.08 m;

- inner radius of the analyzed cylindrical elements, R_i = 0.0445 [m];

- wall thickness of the cylindrical elements, δ_j [m]: $\delta_1 = 0.003\,\text{m}$; $\delta_2 = 0.018\,\text{m}$; $\delta_3 = 0.003\,\text{m}$;

- average radius of the envelope, $R_{mj} = R_i + \delta_j / 2$ [m]: $R_{m\,1} = 0.0460\,\text{m}$; $R_{m\,2} = 0.0454\,\text{m}$; $R_{m\,3} = 0.0460\,\text{m}$;

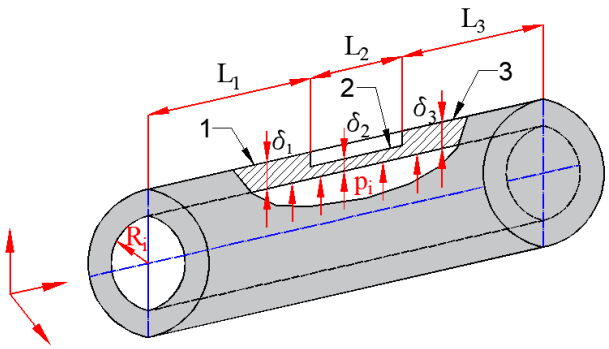

Fig. 1. Model of the geometric structure subjected to analysis

- modulus of longitudinal elasticity of the construction material, $E_1 = E_2 = E_3 = 2.1 \cdot 10^{11} Pa$;

- Poisson's ratio, ν = 0.3;

- the coefficient of cylindrical bending stiffness of the construction elements is calculated according to the relation

$$\Re_{1j} = E \cdot \delta_j^3 / [12 \cdot (1 - \nu^2)][\text{N·m}] \quad (1)$$

$\Re_1 = 5.19 \cdot 10^2$ [N·m]; $\Re_2 = 1.12 \cdot 10^2$ [N·m]; $\Re_3 = 5.19 \cdot 10^2$ [N·m].

- the attenuation coefficient is calculated according to the relation [11]:

$$k_j = \sqrt[4]{3 \cdot (1 - \nu^2)} \Big/ \sqrt{R_{mj} \cdot \delta_j} \quad [1/\text{m}] \quad (2)$$

$k_1 = 1.02 \cdot 10^2$ [1/m]; $k_2 = 1.42 \cdot 10^2$ [1/m]; $k_3 = 1.09 \cdot 10^2$ [1/m].

3. Analytical evaluation of stress-strain states

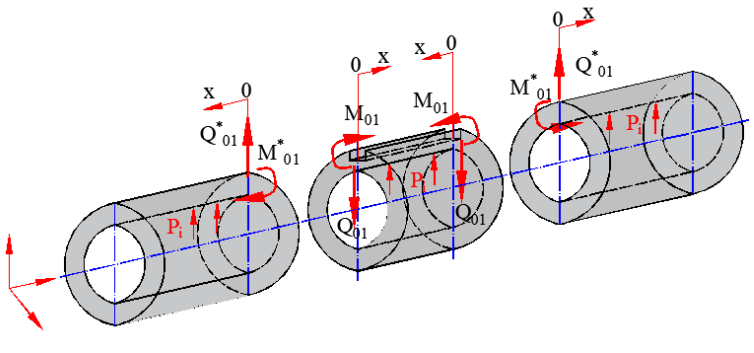

a. b. c.

Fig. 2. Discretization and loading of the analyzed geometrical structure:
a - structural element 1; b) structural element 2; c) - structural element 3

To determine the bond loads (shear forces, Q_{01}, Q_{02} [N/m] and bending moments, M_{01}, M_{02} [N·m/m]) in Fig. 2, the compatibility of the continuity equations of radial displacements and rotations of neighboring elements is used.
The following *study assumptions* are considered:

a. the construction material of the cylindrical sections is considered homogeneous, isotropic and continuous. The stress is considered to be in the elastic domain. The transition between sections of different thicknesses is abrupt (no linear or curved transition);

b. the intermediate section is of constant thickness, smaller than that of the lateral sections. Its length falls into the category of short cylinders with length less than the length of the characteristic half-wave, L_{sc} [11]:

$$L_2 < L_{sc} \approx 12.5 \cdot \sqrt{R_{m2} \cdot \delta_2} \tag{3}$$

c. the plane stress state is used;

d. the radial displacements of elements 1 and 3 have been corrected by bringing them to the values corresponding to the median surface of element 2 (Fig. 2).

3.1. Setting bonding loads

In order to determine the bonding loads, the deformation continuity equations are written, resulting in the linear algebraic system [12]:

$$[A] \cdot \{S_l\} = \{T_l\} \tag{4}$$

where:
- $[A]$ is the non-zero matrix of the influence factors of the bonding loads:

$$[A] = \begin{bmatrix} a_{11} & a_{12} & a_{13} & a_{14} \\ a_{21} & a_{22} & a_{23} & a_{24} \\ a_{31} & a_{32} & a_{33} & a_{34} \\ a_{41} & a_{42} & a_{43} & a_{44} \end{bmatrix}, \tag{5}$$

- $\{S_l\}$ - the transposed matrix of bonding loads:

$$\{S_l\} = \{M_{01} Q_{01} M_{02} Q_{02}\}^T \tag{6}$$

and $\{T_l\}$ - the transposed matrix of free terms:

$$\{T_l\} = \left\{ b_1, b_2, b_3, b_4 \right\}^T \tag{7}$$

From relation (4), the expression of the transpose matrix of the binding loads is derived as:

$$\{S_l\} = \{A\}^{-1} \cdot \{T_l\} \tag{8}$$

where $\{A\}^{-1}$ represents the inverse matrix of influencing factors $\{a_{ij}\}$.

Tables 1 and 2 show the relations for calculating the influence factors $\{a_{ij}\}$ and $\{b_i\}$, respectively, and the values obtained, using the program Mathcad 15.0, for the real model (Fig. 1)**.**

Table 1

Expressions and values of influencing factors

Expressions $\{a_{ij}\}$ (i = 1, 2,….,4; j = 1, 2, …,4) [7]	M.U.	Values obtained
1	2	3
$s_h = 0.5 \cdot \left[exp(k_2 \cdot L_2) - exp(-k_2 \cdot L_2) \right]$	-	611.842
$c_h = 0.5 \cdot \left[exp(k_2 \cdot L_2) + exp(-k_2 \cdot L_2) \right]$	-	611.843
$s = sin(k_2 \cdot L_2)$	-	0.736
$c = cos(k_2 \cdot L_2)$	-	0.678
$N = s_h^2 \cdot (k_2 \cdot L_2) - \sin^2(k_2 \cdot L_2)$	-	$3.743 \cdot 10^5$
$f_{1m} = (s_h^2 + s^2)/N$	-	1
$f_{2m} = -(s \cdot c + s_h \cdot c_h)/N$	-	-1
$f_{1q} = (s \cdot c - s_h \cdot c_h)/N$	-	-1
$f_{2q} = s_h^2/N$	-	1
$f_{3q} = s^2/N$	-	$1.445 \cdot 10^{-6}$
$f_{23q} = f_{2q} + f_{3q}$	-	1
$f_{md} = f_{1m} \cdot c \cdot c_h + f_{2m} \cdot (c \cdot s_h + s \cdot c_h) + s \cdot s_h$	-	$-2.404 \cdot 10^{-3}$
$f_{mr} = f_{1m} \cdot (c \cdot s_h - s \cdot c_h) + 2 \cdot f_{2m} \cdot c \cdot c_h + c \cdot s_h + s \cdot c_h$	-	$-4.619 \cdot 10^{-3}$
$f_{qr} = f_{1q} \cdot (c \cdot s_h - s \cdot c_h) + f_{2q} \cdot (c \cdot c_h - s \cdot s_h) + f_{3q} \cdot (c \cdot c_h + s \cdot s_h)$	-	$2.404 \cdot 10^{-3}$
$f_{qd} = f_{1q} \cdot c \cdot c_h + f_{2q} \cdot c \cdot s_h + f_{3q} \cdot s \cdot s_h$	-	$9.483 \cdot 10^{-5}$
$a_{11} = \frac{1}{2 \cdot k_1^2 \cdot \Re_1} \cdot \frac{R_{m2}}{R_{m1}} + \frac{1}{2 \cdot k_2^2 \cdot \Re_2} \cdot f_{1m}$	m/N	$3.11 \cdot 10^{-7}$
$a_{12} = -\frac{1}{2 \cdot k_1^3 \cdot \Re_1} \cdot \frac{R_{m2}}{R_{m1}} + \frac{1}{2 \cdot k_2^3 \cdot \Re_2} \cdot f_{1q}$	m²/N	$-2.434 \cdot 10^{-9}$
$a_{13} = \frac{1}{2 \cdot k_2^2 \cdot \Re_2} \cdot f_{md}(L_2)$	m/N	$-5.301 \cdot 10^{-10}$
$a_{14} = \frac{1}{2 \cdot k_2^3 \cdot \Re_2} \cdot f_{qd}(L_2)$	m²/N	$1.471 \cdot 10^{-13}$

$a_{2\,1} = \frac{1}{k_1 \cdot \Re_1} \cdot \frac{R_{m\,2}}{R_{m\,1}} + \frac{1}{k_2 \cdot \Re_2} \cdot f_{2\,m}$	1/N	-4.416·10^{-5}
$a_{2\,2} = -\frac{1}{2 \cdot k_1^2 \cdot \Re_1} \cdot \frac{R_{m\,2}}{R_{m\,1}} + \frac{1}{2 \cdot k_2^2 \cdot \Re_2} \cdot f_{2\,3\,q}$	m/N	1.3·10^{-7}
$a_{2\,3} = -\frac{1}{2 \cdot k_2 \cdot \Re_2} \cdot f_{m\,r}\ (L_2)$	1/N	1.448·10^{-7}
$a_{2\,4} = -\frac{1}{2 \cdot k_2^2 \cdot \Re_2} \cdot f_{q\,r}\ (L_2)$	m/N	-5.301·10^{-10}
$a_{3\,1} = \frac{1}{2 \cdot k_2^2 \cdot \Re_2} \cdot f_{m\,d}\ (L_2)$	m/N	-5.301·10^{-10}
$a_{3\,2} = \frac{1}{2 \cdot k_2^3 \cdot \Re_2} \cdot f_{q\,d}\ (L_2)$	m^2/N	1.471·10^{-13}
$a_{3\,3} = \frac{1}{2 \cdot k_3^2 \cdot \Re_3} \cdot \frac{R_{m\,2}}{R_{m\,3}} + \frac{1}{2 \cdot k_2^2 \cdot \Re_2} \cdot f_{1\,m}$	m/N	2.999·10^{-7}
$a_{3\,4} = -\frac{1}{2 \cdot k_3^2 \cdot \Re_3} \cdot \frac{R_{m\,2}}{R_{m\,3}} + \frac{1}{2 \cdot k_2^3 \cdot \Re_2} \cdot f_{1\,q}$	m^2/N	-2.276·10^{-9}
$a_{4\,1} = \frac{1}{2 \cdot k_2 \cdot \Re_2} \cdot f_{m\,r}(L_2)$	1/N	-1.448·10^{-7}
$a_{4\,2} = -\frac{1}{2 \cdot k_2^2 \cdot \Re_2} \cdot f_{q\,r}(L_2)$	m/N	-5.301·10^{-10}
$a_{4\,3} = \frac{1}{k_3 \cdot \Re_3} \cdot \frac{R_{m\,2}}{R_{m\,3}} + \frac{1}{k_2 \cdot \Re_2} \cdot f_{2\,m}$	1/N	-4.533·10^{-5}
$a_{4\,4} = -\frac{1}{2 \cdot k_3^2 \cdot \Re_3} \cdot \frac{R_{m\,2}}{R_{m\,3}} + \frac{1}{2 \cdot k_2^3 \cdot \Re_2} \cdot f_{2\,3\,q}$	m/N	-7.783·10^{-8}

Table 2

Expressions and values of the elements of the transposed matrix of free terms

Expressions $\{b_i\}$ (i = 1, 2,….,4) [7]	M.U.	Values obtained
1	2	3
$b_1 = \frac{p_i}{1\,6} \cdot \left[\frac{R_{m\,2}}{k_1^4 \cdot \Re_1 \cdot R_{m\,1}} - \frac{1}{k_2^4 \cdot \Re_2} - \nu \cdot R_i^2 \cdot \left(\frac{1}{k_1^4 \cdot \Re_1 \cdot R_{m\,1}^2} - \frac{1}{k_2^4 \cdot \Re_2 \cdot R_{m\,2}^2} \right) \right]$	m	$-5.982 \cdot 10^{-7}$
$b_2 = 0$	-	
$b_3 = \frac{p_i}{1\,6} \cdot \left[\frac{R_{m\,2}}{k_3^4 \cdot \Re_3 \cdot R_{m\,3}} - \frac{1}{k_2^4 \cdot \Re_2} - \nu \cdot R_i^2 \cdot \left(\frac{1}{k_3^4 \cdot \Re_3 \cdot R_{m\,3}^2} - \frac{1}{k_2^4 \cdot \Re_2 \cdot R_{m\,2}^2} \right) \right]$	m	$-1.132 \cdot 10^{-6}$
$b_4 = 0$	-	

According to relation (7), the *values of the bond loads* (shear stress and bending moments) result:

$M_{01} = 1.149\ \text{N}\cdot\text{m/m}$;

$Q_{01} = 392.821\ \text{N/m}$;

$M_{02} = -0,703\ \text{N}\cdot\text{m/m}$;

$Q_{02} = 404.484\ \text{N/m}$.

3.2. Determination of stress states

The meridional stresses $\sigma_{1t}(x)$ and annular stresses $\sigma_{2t}(x)$ developed in cylindrical elements 1 and 3, under the action of internal pressure, are calculated with the relations [12]:

$$\sigma_{1\,t}(x) = \frac{p_i \cdot R_{mt}}{2 \cdot \delta_t} \pm \frac{6 \cdot M_t(x)}{\delta_t^2} \tag{9}$$

$$\sigma_{2\,t}(x) = \frac{p_i \cdot R_{mt}}{\delta_t} \pm \frac{6 \cdot \nu \cdot M_t(x)}{\delta_t^2} \tag{10}$$

where, t represents the number of the construction element (t = 1, 3 - Fig. 2), $M_t(x)$ - the meridional bending moment, developed by the unit forces Q_{01}, Q_{02} and the bending moments M_{01}, M_{02} (Fig. 2), which is calculated with the relation [12]:

$$M_t(x) = \left[\frac{1}{k_t} \cdot Q_{0t} \cdot s_{tex} - M_{0t}(c_{tex} + s_{tex})\right] \cdot \frac{R_{m2}}{R_{mt}} \tag{11}$$

In relations (9) and (10) the sign "+" is considered for the inner surfaces and the sign "- " for the outer surfaces.

The current dimension x, for cylindrical elements 1 and 3, is always zero in the plane of separation from cylindrical element 2 and is measured along the generator, characteristic of each cylindrical element 1 and 3.

The meridional stress $\sigma_{12}(x)$ and the annular stress $\sigma_{22}(x)$, corresponding to the cylindrical element 2 (Fig. 2), are calculated with the relations [7]:

$$\sigma_{1\,2}(x) = \frac{p_i \cdot R_{m\,2}}{2 \cdot \delta_2} \pm \frac{6 \cdot M_{2\,x}(x, M_{01}, M_{02})}{\delta_2^2} \mp \frac{6 \cdot M_{2\,x}(x, Q_{01}, Q_{02})}{\delta_2^2} \tag{12}$$

$$\sigma_{2\,2}(x) = \frac{p_i \cdot R_{m\,2}}{\delta_2} \pm \frac{6 \cdot K_{2\,x}(x, M_{01}, M_{02})}{\delta_2^2} \mp \frac{6 \cdot K_{2\,x}(x, Q_{01}, Q_{02})}{\delta_2^2} + \frac{T_{2\,x}(x, M_{01}, M_{02})}{\delta_2} + \frac{T_{2\,x}(x, Q_{01}, Q_{02})}{\delta_2}. \tag{13}$$

where $T_t(x)$ is the annular force:

$$T_t(x) = 2\,[Q_{0t} \cdot c_{tex} - k_t\, M_{0t}(c_{tex} + s_{tex})] \cdot k_t R_{m2} \tag{14}$$

respectively:

$$s_{tex} = exp(-k_t \cdot x) \cdot sin(k_t \cdot x) \tag{15}$$

$$c_{tex} = exp(-k_t \cdot x) \cdot cos(k_t \cdot x) \tag{16}$$

In relations (12) and (13) the sign "+" for the bending moments $M_{2x}(x, M_{o1}, M_{o2})$, $K_{2\,x}(x,\ M_{0\,1},\ M_{0\,2})$ and the sign '- ' for the unit bending moments $M_{2x}(x, Q_{o1}, Q_{o2})$, $K_{2\,x}(x,\ Q_{0\,1},\ Q_{0\,2})$ are characteristic of the inner surface of the cylindrical element 2.

The following notations have been used: $M_{2x}(x, M_{o1}, M_{o2}) = M_{2xM}$, $M_{2x}(x, Q_{o1}, Q_{o2}) = M_{2xQ}$, $T_{2x}(x, M_{o1}, M_{o2}) = T_{2xM}$, $T_{2x}(x, Q_{o1}, Q_{o2}) = T_{2xQ}$.

Table 3 shows their computational relations and the values obtained using the program Mathcad 15.0, for the current dimension $x = 0$.

The *von Mises equivalent stresses* are calculated with the formula [11,12]:

$$\sigma_{ech}^{IV} = \sqrt{\sigma_{1j}^2 + \sigma_{2j}^2 - \sigma_{1j} \cdot \sigma_{2j}} \tag{17}$$

Table 3

Notations in stress expressions

Notation definition	M.U.	Values obtained
1	2	3
$K_{2x}(x, M_{01}, M_{02}) = \nu \cdot M_{2x}(x, M_{01}, M_{02})$	N·m/m	$-1.917 \cdot 10^{-13}$
$K_{2x}(x, Q_{01}, Q_{02}) = \nu \cdot M_{2x}(x, Q_{01}, Q_{02})$	N·m/m	$-4.711 \cdot 10^{-11}$
$M_{2xM} = M_{01} \cdot \left[\begin{array}{c} -f_{1m} \cdot s_{k_2 x} \cdot s_{h\,k_2 x} + \\ +f_{2m} \cdot \left(c_{k_2 x} \cdot s_{h\,k_2 x} - s_{k_2 x} \cdot c_{h\,k_2 x} \right) + \\ + c_{k_2 x} \cdot c_{h\,k_2 x} \end{array} \right] +$	N·m/m	$-639.06 \cdot$ $\cdot 10^{-15}$

$+M_{02}\cdot\begin{Bmatrix} -f_{1m}\cdot s_{k_2 L_2 x}\cdot s_{h k_2 L_2 x}+ \\ f_{2m}\cdot\begin{bmatrix} c_{k_2 L_2 x}\cdot s_{h k_2 L_2 x}- \\ -s_{k_2 L_2 x}\cdot c_{h k_2 L_2 x} \end{bmatrix}+ \\ +c_{k_2 L_2 x}\cdot c_{h k_2 L_2 x} \end{Bmatrix}$		
$M_{2xQ}=\frac{1}{k_2}\cdot Q_{01}\cdot\begin{pmatrix} -f_{1q}\cdot s_{k_2 x}\cdot s_{h k_2 x}- \\ -f_{2q}\cdot s_{k_2 x}\cdot c_{h k_2 x}+ \\ +f_{3q}\cdot c_{k_2 x}\cdot s_{h k_2 x} \end{pmatrix}+$ $+\frac{1}{2}\cdot Q_{02}\cdot\begin{bmatrix} -f_{1q}\cdot s_{k_2 L_2 x}\cdot s_{h k_2 L_2 x}- \\ -f_{2q}\cdot s_{k_2 L_2 x}\cdot c_{h k_2 L_2 x}+ \\ +f_{3q}\cdot c_{k_2 L_2 x}\cdot s_{h k_2 L_2 x} \end{bmatrix}$	N·m/m	$-1.57\cdot 10^{-10}$
$T_{2xM}=2\cdot k_2^2\cdot R_{m2}\cdot\{ M_{01}\cdot\begin{bmatrix} f_{1m}\cdot c_{k_2 x}\cdot c_{h k_2 x}+ \\ +f_{2m}\cdot\begin{pmatrix} c_{k_2 x}\cdot s_{h k_2 x} \\ +s_{k_2 x}\cdot c_{h k_2 x} \end{pmatrix}+ \end{bmatrix}$ $+s_{k_2 x}\cdot s_{h k_2 x}\Big]+M_{02}\cdot\begin{bmatrix} f_{1m}\cdot c_{k_2 L_2\cdot x}\cdot c_{h k_2 L_2 x}+ \\ +f_{2m}\cdot\begin{pmatrix} c_{k_2 L_2\cdot x}\cdot s_{h k_2 L_2 x}+ \\ +s_{k_2 L_2\cdot x}\cdot c_{h k_2 L_2 x} \end{pmatrix} \\ +s_{k_2 L_2\cdot x}\cdot c_{h k_2 L_2 x} \end{bmatrix}$	N·m/m	16.538
$T_{2xQ}=-2\cdot k_2\cdot R_{m2}\cdot[Q_{01}\cdot\begin{pmatrix} f_{1q}\cdot c_{k_2 x}\cdot c_{h k_2 x}+ \\ +f_{2q}\cdot c_{k_2 x}\cdot s_{h k_2 x}+ \\ +f_{3q}\cdot s_{k_2 x}\cdot c_{h k_2 x} \end{pmatrix}+$	N·m/m	-3.521

$+Q_{02}\cdot\left[\begin{array}{l} f_1 q^{\cdot c} k_2 L_2 x^{\cdot c} h k_2 L_2 x + \\ +f_2 q^{\cdot c} k_2 L_2 x^{\cdot s} h k_2 L_2 x + \\ +f_3 q^{\cdot s} k_2 L_2 x^{\cdot c} h k_2 L_2 x \end{array}\right]$		

4. Experimental evaluation of stress-strain states

The study presents the experimental results obtained from the tests carried out on the model shown in Fig. 1, subjected to an internal pressure, using electro-resistive tensiometry.

The transducers were placed as shown in Fig. 3.

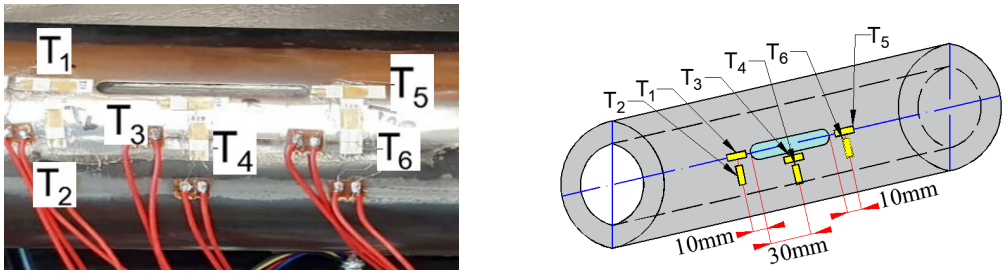

a. b.

Fig. 3. Experimental model (a); positioning of the electro-tensometric transducers (b).

Electro-resistive tensometry was used to practically determine the mechanical stress state of the analyzed technical system, as it allows the measurement of specific linear deformations in several directions and the application of analytical formulas corresponding to the theory of elasticity [13-15].

4.1. Experimental research method

For the experiments was used the experimental set up shown in Fig. 4, which includes, in addition to the model in Fig. 1, other equipment and accessories: data acquisition system MGCPlus (with 40 measuring points), pump with pressure gauge, Lenovo laptop (with specialized software Catman Easy, necessary for data acquisition and processing of test results) and electro-tensiometric marks (with foil type 6/120 LY 11, manufactured by Hottinger).

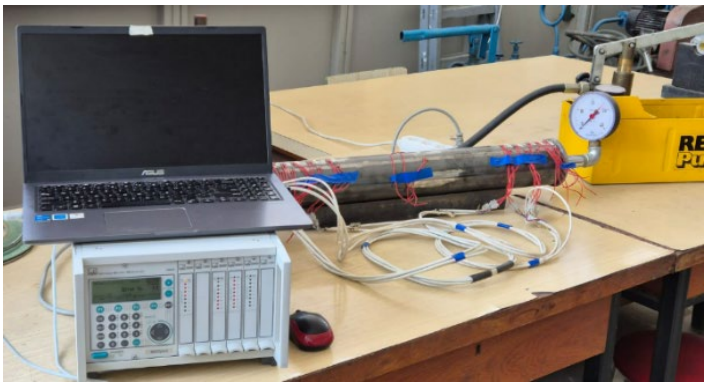

Fig. 4. The experimental stand

Specific linear strains in the meridional direction (ε_{1j} [μm/m]) and in the annular direction (ε_{2j} [μm/m]) were measured with electro-tensiometric transducers at an internal pressure p_i = 3 MPa.

4.2. Results of experimental research

The values of the stresses σ_{1j} and σ_{2j}, calculated based on the specific deformations, are as follows [8-10]:

$$\sigma_{1j} = \frac{E}{1-\nu^2} \cdot \left(\varepsilon_{1j} + \nu \cdot \varepsilon_{2j} \right) [MPa] \tag{18}$$

$$\sigma_{2j} = \frac{E}{1-\nu^2} \cdot \left(\varepsilon_{2j} + \nu \cdot \varepsilon_{1j} \right) [MPa], \tag{19}$$

where E is the longitudinal modulus of elasticity (Young's modulus); ν - the coefficient of transverse contraction (Poisson's ratio); ε1j and ε2j - the specific linear strains normal to the principal directions, in μm/m.

The equivalent stresses are calculated with relation (17).

5. Results and discussions

After carrying out the calculations using the analytical relations presented previously (4-17), the values of the equivalent stresses corresponding to the inner (with index "i") and outer (with index "e") surfaces of the analyzed construction elements along the length of each element were obtained (Table 4). The direction of the Ox axis for each element is as shown in Figure 2.

Table 4

Values of equivalent stresses obtained analytically

x [mm] / The element	0	10	20	30	40	50
1	$\sigma_{11\,i} = 22.24$	$\sigma_{11\,i} = 23.40$	$\sigma_{11\,i} = 23.25$	$\sigma_{11\,i} = 23.04$	$\sigma_{11\,i} = 22.98$	$\sigma_{11\,i} = 22.99$
	$\sigma_{11\,e} = 23.76$	$\sigma_{11\,e} = 22.60$	$\sigma_{11\,e} = 22.75$	$\sigma_{11\,e} = 22.96$	$\sigma_{11\,e} = 23.02$	$\sigma_{11\,e} = 23.01$
	$\sigma_{21\,i} = 46.63$	$\sigma_{21\,i} = 46.39$	$\sigma_{21\,i} = 46.07$	$\sigma_{21\,i} = 45.97$	$\sigma_{21\,i} = 45.98$	$\sigma_{21\,i} = 46.00$
	$\sigma_{21\,e} = 47.08$	$\sigma_{21\,e} = 46.15$	$\sigma_{21\,e} = 45.92$	$\sigma_{21\,e} = 45.95$	$\sigma_{21\,e} = 45.99$	$\sigma_{21\,e} = 46.00$
	$\sigma_{ech\,i} = 40.44$	$\sigma_{ech\,i} = 40.18$	$\sigma_{ech\,i} = 39.90$	$\sigma_{ech\,i} = 39.81$	$\sigma_{ech\,i} = 39.82$	$\sigma_{ech\,i} = 39.84$
	$\sigma_{ech\,e} = 40.77$	$\sigma_{ech\,e} = 39.97$	$\sigma_{ech\,e} = 39.77$	$\sigma_{ech\,e} = 39.79$	$\sigma_{ech\,e} = 39.83$	$\sigma_{ech\,e} = 39.84$
2	$\sigma_{12\,i} = 37.83$	$\sigma_{12\,i} = 35.33$	$\sigma_{12\,i} = 37.30$	$\sigma_{12\,i} = 38.97$	$\sigma_{12\,i} = 38.13$	$\sigma_{12\,i} = 37.83$
	$\sigma_{12\,e} = 37.83$	$\sigma_{12\,e} = 40.34$	$\sigma_{12\,e} = 38.36$	$\sigma_{12\,e} = 36.70$	$\sigma_{12\,e} = 37.54$	$\sigma_{12\,e} = 37.83$
	$\sigma_{22\,i} = 75.67$	$\sigma_{22\,i} = 74.92$	$\sigma_{22\,i} = 75.49$	$\sigma_{22\,i} = 76.02$	$\sigma_{22\,i} = 75.79$	$\sigma_{22\,i} = 75.64$
	$\sigma_{22\,e} = 75.67$	$\sigma_{22\,e} = 76.42$	$\sigma_{22\,e} = 75.81$	$\sigma_{22\,e} = 75.34$	$\sigma_{22\,e} = 75.61$	$\sigma_{22\,e} = 75.64$
	$\sigma_{ech\,i} = 65.53$	$\sigma_{ech\,i} = 64.92$	$\sigma_{ech\,i} = 65.38$	$\sigma_{ech\,i} = 65.84$	$\sigma_{ech\,i} = 65.64$	$\sigma_{ech\,i} = 65.51$
	$\sigma_{ech\,e} = 65.53$	$\sigma_{ech\,e} = 66.22$	$\sigma_{ech\,e} = 65.65$	$\sigma_{ech\,e} = 65.25$	$\sigma_{ech\,e} = 65.48$	$\sigma_{ech\,e} = 65.51$
3	$\sigma_{13\,i} = 23.46$	$\sigma_{13\,i} = 23.93$	$\sigma_{13\,i} = 23.23$	$\sigma_{13\,i} = 22.97$	$\sigma_{13\,i} = 22.96$	$\sigma_{13\,i} = 22.99$
	$\sigma_{13\,e} = 22.54$	$\sigma_{13\,e} = 22.07$	$\sigma_{13\,e} = 22.77$	$\sigma_{13\,e} = 23.03$	$\sigma_{13\,e} = 23.04$	$\sigma_{13\,e} = 23.01$
	$\sigma_{23\,i} = 46.14$	$\sigma_{23\,i} = 46.28$	$\sigma_{23\,i} = 46.07$	$\sigma_{23\,i} = 45.99$	$\sigma_{23\,i} = 45.99$	$\sigma_{23\,i} = 46.00$
	$\sigma_{23\,e} = 47.46$	$\sigma_{23\,e} = 45.89$	$\sigma_{23\,e} = 45.80$	$\sigma_{23\,e} = 45.95$	$\sigma_{23\,e} = 46.01$	$\sigma_{23\,e} = 46.01$
	$\sigma_{ech\,i} = 39.96$	$\sigma_{ech\,i} = 40.09$	$\sigma_{ech\,i} = 39.90$	$\sigma_{ech\,i} = 39.83$	$\sigma_{ech\,i} = 39.83$	$\sigma_{ech\,i} = 39.84$
	$\sigma_{ech\,e} = 41.12$	$\sigma_{ech\,e} = 39.75$	$\sigma_{ech\,e} = 39.66$	$\sigma_{ech\,e} = 39.79$	$\sigma_{ech\,e} = 39.85$	$\sigma_{ech\,e} = 39.85$

Figure 5 has graphically plotted the variation of equivalent stress at both the inner and outer surface along the length of elements 1, 2 and 3. It can be seen that at both the inside and outside, the stress decreases along the half-wavelength.

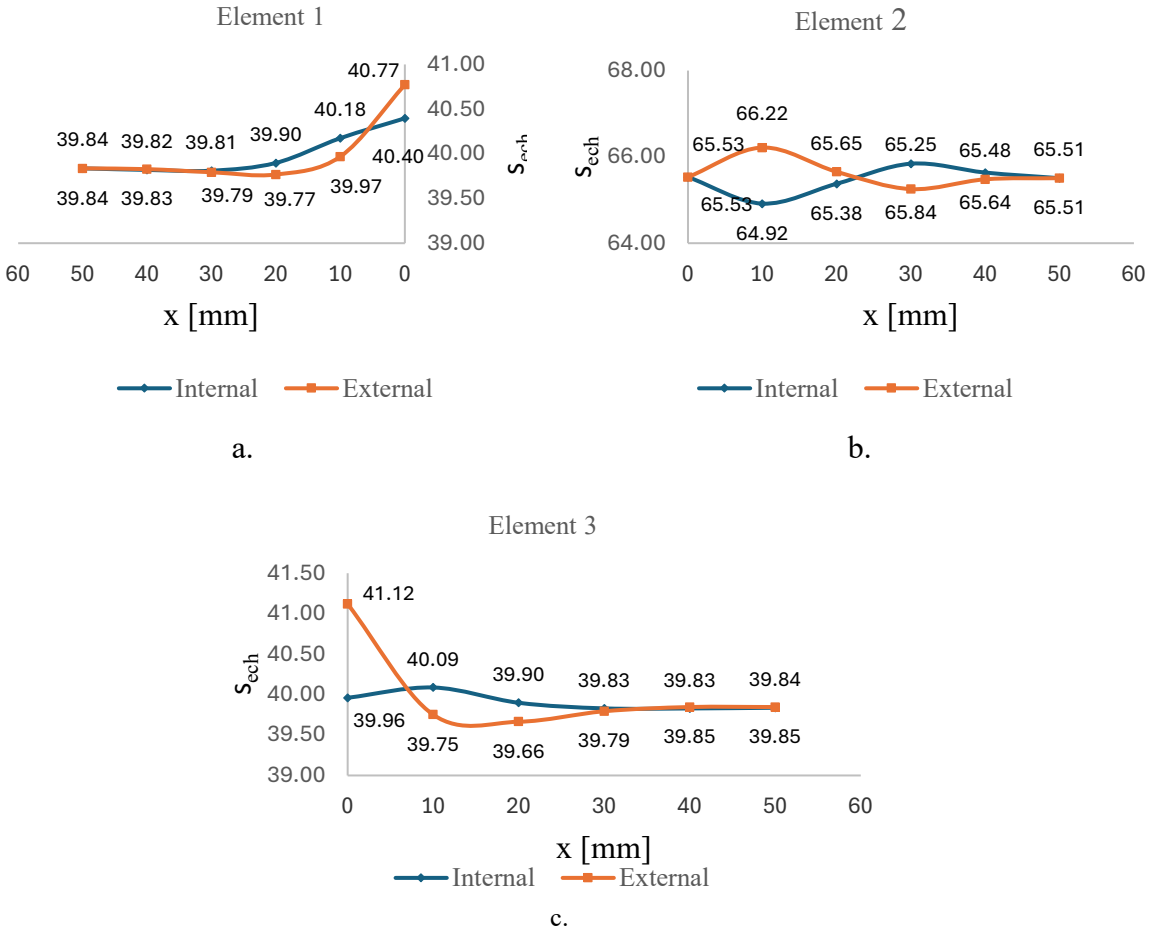

Fig. 5. Equivalent stress variation along x
a. Element 1; b. Element 2; c. Element 3

Table 5 shows the values of the experimental specific strains measured externally, the stresses in the meridional and annular directions, as well as the equivalent stresses (relations 18 - 20) in the transducer zones (fig. 3).

Table 5

Values of experimental specific strains and stress

i	ε_{ri} [μm/m]	j	ε_{cj} [μm/m]	σ_{1i} [MPa]	σ_{1j} [MPa]	$\sigma_{ech,\exp}$ [MPa]
1	22.94	2	118.83	13.52	29.01	25.14
2	61.37	4	120.72	22.52	32.11	28.55
3	26.07	6	128.77	14.93	31.52	27.31

The values of the equivalent stresses, determined both analytically and experimentally, were compared with the allowable strength of the construction material, σ_a = 176 MPa. In all cases the equivalent stresses are lower than the allowable strength.

After processing the analytical and experimental results of the equivalent stresses (σ_{ech} and $\sigma_{ech,\exp}$), for the cylindrical elements (1, 2 and 3), specific to the analyzed models on the outer surfaces, differences in the obtained results resulted (Table 6).

Table 6

Analytical and experimental stresses

Element 1 x=10 mm	σ_{ech} = 39.97 MPa	$\sigma_{ech,exp}$ = 25.14 MPa
Element 2 x=30 mm	$\boldsymbol{\sigma_{ech}} = \mathbf{65.25}$ MPa	$\boldsymbol{\sigma_{ech,exp}} = \mathbf{28.55}$ MPa
Element 3 x=10 mm	$\boldsymbol{\sigma_{ech}} = \mathbf{39.75}$ MPa	$\boldsymbol{\sigma_{ech,exp}} = \mathbf{27.31}$ MPa

These differences are motivated, on the one hand, by the fact that the construction material of the model (PG265GH) is not homogeneous, isotropic and continuous - as considered in the hypotheses of the analytical study, and on the other hand, due to the consideration of element 2 of the analytical model which does not have an axial-symmetric geometrical structure.

Also, another cause of the differences between the above-mentioned results is the consideration in the analytical study only of the effect of internal pressure, while the experimental part was carried out under real conditions, having also an external pressure - atmospheric pressure.

The difference between the equivalent stresses calculated with the analytical method and those measured experimentally, in percentage, is as follows: 37.10% for element 1; 56.25% for element 2 and 31.30% for element 3.

6. Conclusions

The analytical investigation considered the connection between two long cylindrical elements and a short, intermediate cylindrical element. The deformation continuity equations were established, so that on the basis of the linear algebraic system, the expressions for the connection loads Q_{01}, Q_{02}, M_{01}, M_{02}. were obtained. With their help, were written the relations of the meridional and annular strains in the case of the plane state of strains, dependent on the x coordinate.

For the accepted strength theory, the 4th strength theory, the equivalent stresses at the interior and exterior surfaces of the analyzed elements have been determined to be less than the allowable strength of the construction material.

The presented calculation method can also be used in case the transitions from one structure to another are spliced or linear transitions.

To reduce the difference obtained by applying both methods in the area of the geometrical discontinuity of the cylindrical shell, the use of the actual operating conditions of the analyzed model is considered.

REFERENCES

[1]. *V.V. Jinescu, Vali – Ifigenia Nicolof, Angela Chelu, Nicoleta Teodorescu*, Rezistenţa elementelor tubulare şi a învelişurilor prevăzute cu racorduri tubulare (Strength of tubular components and shells-tubular junction), Proceedings of the 10th Annual Conference of the ASTR, 2015, https://www.agir.ro/buletine/2595.pdf.

[2]. *V.V. Jinescu, Vali – Ifigenia Nicolof*, Proiectarea echipamentelor sub presiune cu considerarea deteriorării produsă de fisuri (Design of pressure equipment with consideration of crack damage), Bulletin AGIR, Supliment 2, 2015.

[3]. *V.V. Jinescu, Vali – Ifigenia Nicolof, Angela Chelu, Simona - Eugenia Manea*, Critical Stresses, Critical Groups Of Stresses And Strengths Of Tubular Structures Without And With Cracks, **U.P.B. Sci. Bull., Series D,** Vol. 77, Iss. 4, 2015, ISSN 1454-2358.

[4]. *V.V. Jinescu, Angela Chelu Vali – Ifigenia Nicolof, Georgeta Roman (Urse),* Strength Analysis Of Shells On The Basis Of Principle Of Critical Energy, **U.P.B. Sci. Bull., Series D**, Vol. 81, Iss. 3, 2019, ISSN 1454-2358.

[5]. *V.V. Jinescu, Vali – Ifigenia Nicolof, C. Jinescu, Angela Chelu,* Superposition of Effects in Calculating the Deterioration of Tubular Structures and in Non-newtonian Fluid Flow*,* Rev. Chim., Vol. 66, Year: 2015, Iss. 5, 2015, http://www.revistadechimie.ro.

[6]. *N. Zhangabay, U. Suleimenov, A. Utelbayeva, Svetlana Buganova, A. Tolganbayev, Karshyga Galymzhan, S. Dossybekov, K. Baibolov, R. Fediuk, M. Amran, B. Duissenbekov, A. Kolesnikov,* Experimental research of the stress-strain state of prestressed cylindrical shells taking into account temperature effects, Case Studies in Construction Materials 18, 2023, https://doi.org/10.1016/j.cscm.2022.e01776.

[7]. *V.G. Belardi, M. Ottaviano, F. Vivio,* Bending theory of composite pressure vessels: A closed-form analytical approach, Composite Structures 329, 117799, (2024), https://doi.org/10.1016/j.compstruct.2023.117799

[8]. *A. Demyanov*, Quasistatic evolution in the theory of perfect elasto-plastic plates. Part II: Regularity of bending moments, L'Association Publications de l'Institut Henri Poincaré. Published by Elsevier B.V., (2009), https://doi:10.1016/j.anihpc

[9]. *H. Yousfi, M. Brioua, R. Benbouta,* Study And Prediction Of The Fatigue Life Of Aisi 1045 Steel Structures Under Rotational Bending Stresses, **U.P.B. Sci. Bull., Series D**, Vol. 84, Iss. 2, 2022, ISSN 1454-2358.

[10]. *Șt. Culafic, D. Bajic, T. Maneski*, Experimental research of stress state and residual stresses of the hydropower pipeline branch model, International Journal of Pressure Vessels and Piping, Published by Elsevier Ltd, (2023), https://doi.org/10.1016/j.ijpvp.2023.105089

[11]. *G.C. Ciocoiu, R.I. Iatan, Nicoleta Sporea, I. Durbacă, I. Cherciu,* Studiul analitic al stărilor de solicitare într-o placă circulară plană, cu extindere restrânsă și cu racord central (Analitical study of stress states in a plane circular plate with restricted expansion, and a central connection), Synthesis of theoretical and applied mechanics, Published by Matrix Rom, Vol. 15, Nr. 1, Bucharest, 2024, pp. 23-36, ISSN 2068-6331.

[12]. *I. R. Iatan, C. Gh. Ciocoiu, Mădălina-Anca Dumitrescu*, Evaluation of stress states in areas with geometric structure discontinuities in the configuration of pressure equipment. I. Direct discontinuity, Hidraulica, nr. 2, 2023, p. 48 – 55 (ISSN 1453 – 7303).

[13]. *** ASME Boiler and Pressure Vessel Code. Section VIII, Division 2, Rules for construction of pressure vessels, 2010.
[14]. *** EN 1591, Flanges and their joints - Design rules for gasketed circular flange connections - Part 1: Calculation method, 2014.
[15]. *H. Estrada,* Analysis of leakage in bolted flanged joints using contact finite element analysis, Journal of Mechanics Engineering and Automation, vol. 5, nr. 3, 2015, p. 135 – 142.